Carbohydrate Polymers 123 (2015) 130–135

Contents lists available at ScienceDirect

Carbohydrate Polymers

journal homepage: www.elsevier.com/locate/carbpol

^{13}C and ^{15}N solid-state NMR studies on albendazole and cyclodextrin albendazole complexes

M. João G. Ferreira[a], A. García[b], D. Leonardi[b], Claudio J. Salomon[b], M. Celina Lamas[b,*], Teresa G. Nunes[a,**]

[a] CQE, Instituto Superior Técnico, Universidade de Lisboa, Av. Rovisco Pais, 1049-001 Lisboa, Portugal
[b] IQUIR-CONICET, Facultad de Ciencias Bioquímicas y Farmacéuticas, Área Técnica Farmacéutica, Universidad Nacional de Rosario, Rosario, Argentina

ARTICLE INFO

Article history:
Received 1 December 2014
Received in revised form 10 January 2015
Accepted 19 January 2015
Available online 25 January 2015

Keywords:
Albendazole
Cyclodextrin
Inclusion complex
Solid-state NMR

ABSTRACT

^{13}C and ^{15}N solid-state nuclear magnetic resonance (NMR) spectra were recorded from albendazole (ABZ) and from ABZ:β-cyclodextrin, ABZ:methyl-β-cyclodextrin, ABZ:hydroxypropyl-β-cyclodextrin and ABZ:citrate-β-cyclodextrin, which were prepared by the spray-drying technique. ABZ signals were typical of a crystalline solid for the pure drug and of an amorphous compound obtained from ABZ:cyclodextrin samples. Relevant spectral differences were correlated with chemical interaction between ABZ and cyclodextrins. The number and type of complexes revealed a strong dependence on the cyclodextrin group substituent. Solid-state NMR data were consistent with the presence of stable inclusion complexes.

1. Introduction

Cyclodextrins (CDs) are cyclic oligosaccharides derived from starch that have been employed as excipients in pharmaceutical and cosmetic industries because of their ability to interact with poorly water soluble compounds and bring them into aqueous solution. The effect of orally administered drugs is considerably dependent on the dissolution rate of the pharmaceutical drug since it determines its absorption by the gastrointestinal tract (Carrier, Miller, & Ahmed, 2007; Garcíía, Bolás, & Torrado, 2003; Lopez-Garcia, Torrado-Duran, Torrado-Duran, Martínez-Fernández, & Bolás-Fernández, 1997). The more soluble the drug is, the higher its bioavailability and therefore therapeutical action (Brewster & Loftsson, 2007). Drug-CD complexes have therefore been used in liquid and solid formulations for oral administration to improve therapeutical action of non-water soluble drugs in an economical way (Vogt & Strohmeier, 2012).

Albendazole (ABZ, Scheme 1), methyl [5-(propylthio)-1-H-benzimidazol-2-yl] carbamic acid methyl ester, patented in 1975, is one of the most effective broad-spectrum anthelmintic agents (Barrera et al., 2010; Cook, 1990; García et al., 2013). This benzimidazole derivative is particularly effective in the treatment of intestinal helminthiasis but the therapeutic response is unpredictable due to its poor bioavailability (Ahmadnia, Moazeni, Mohammadi-Samani, & Oryan, 2013). It is almost insoluble in water (1 μg/mL) (García et al., 2013), a fact that has been of major concern regarding the preparation of ABZ formulations. Moreover, the solubility decreases by increasing the solution pH (Kohri, Yamayoshi, Iseki, Sato, & Miyazaki, 1998). ABZ:β-CD complexes are among the several approaches that have been used to improve the physicochemical properties of ABZ.

ABZ forms colorless crystals, with melting point between 481 K and 483 K. Two ABZ polymorphs were identified. ABZ Form I (metastable at ambient temperature) is assigned to the commercialized drug, and ABZ Form II, whose crystal structure was determined; Form II is enantiotropically related to Form I but both forms are physically stable owing to high-energy barrier required for the activation of the interconversion (Pranzo, Cruickshank, Coruzzi, Caira, & Bettini, 2010). On the origin of the polymorphism are the possibility of different conformations of the groups attached to the benzimidazole ring (Scheme 1), of tautomers (see also Scheme 1), molecular disorder and the possibility of different hydrogen bonding arrangements between molecules in the unit cell. Charge distribution, enthalpy of formation, dipole moment, and molecular volume were calculated using semiempirical AM1 method for some conformers shown in Scheme 1: b, c, d and e. It was reported that negative charge distributions are localized on the nitrogen of the aromatic ring, the carbonyl group of the carbamoyl moiety and the ester oxygen, whereas positive charge distributions are localized on the proton of the amide group and the proton of the

* Corresponding author.
** Corresponding author. Tel.: +351 21 8419043; fax: +351 21 8464455.
E-mail addresses: mlamas@fbioyf.unr.edu.ar (M.C. Lamas), teresa.nunes@ist.utl.pt (T.G. Nunes).

http://dx.doi.org/10.1016/j.carbpol.2015.01.031
0144-8617/

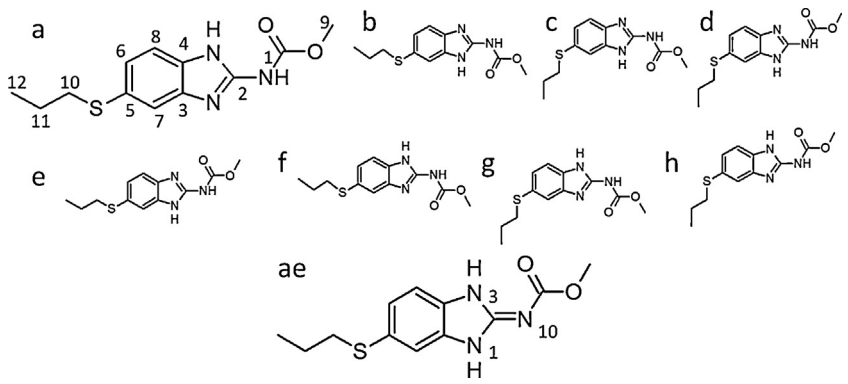

Scheme 1. Chemical structures of some of the possible conformations of the groups attached to the benzimidazole ABZ ring (a–h). The following structures represent pairs of tautomers: a and e, b and f, c and g, d and h. Another tautomer of a and e is also shown (ae).

amine group on the aromatic ring. Based on these data it was suggested that ABZ can participate in both inter- and intramolecular hydrogen bonding and that the contribution of the different structures will depend on the interactions of ABZ with its environment (Fernández, Sigal, Otero, Silber, & Santo, 2011).

Previous studies showed that of all the cyclodextrins tested, citrate-β-CD is the most effective in the solubilization of ABZ. The formation of a stable ABZ:citrate-β-CD inclusion complex (1:1 molar ratio) was confirmed by high resolution mass spectrometry. Solution NMR spectra showed that the tail and the aromatic ring of ABZ were inside the cavity of citrate-β-CD which suggests that the stability of the complex is due to an interaction between the acidic groups of the host and the ABZ basic groups. Based on these results, it was concluded that citrate-β-CD was a suitable excipient to design oral ABZ dosage forms (García, Leonardi, Salazar & Lamas, 2014).

Powder X-ray diffraction of ABZ:citrate-β-CD showed loss of crystallinity upon inclusion but nothing else is known about the solid complex. So far, ABZ:β-CDs systems have not been studied by solid-state NMR (ss-NMR). Hence, the main goal of this study is to obtain evidence on the potential inclusion complexes formed, using that non-destructive technique. The advantages of using ss-NMR in biomedical and pharmaceutical research were recently reviewed (Paradowska & Wawer, 2014). In particular, the inclusion of several drugs (e.g. diflunisal and prednisolone) within the CD cavity was demonstrated using 2D multinuclear ss-NMR (Vogt & Strohmeier, 2012).

2. Materials and methods

2.1. Materials

ABZ, β-CD, hydroxypropyl-β-CD (estimated mol wt. ~1396, average degree of substitution 0.9; HP-β-CD), and methyl-β-CD (estimated mol wt. ~1310, average degree of substitution 1.8; Me-β-CD) were purchased from Sigma-Aldrich (Milwaukee, WI, USA). Citrate-β-CD (estimated mol wt. ~1308, average degree of substitution 1) was synthesized following the route previously described (García, Leonardi, Salazar et al., 2014a)

All other chemicals and solvents used in this study were of analytical reagent grade.

2.2. Methods

2.2.1. Preparation of the inclusion complexes

The inclusion complexes of ABZ with β-CD, HP-β-CD, Me-β-CD and citrate-β-CD (1:1 molar ratio) were prepared as previously described (García, Leonardi, Salazar et al., 2014a; García, Leonardi,

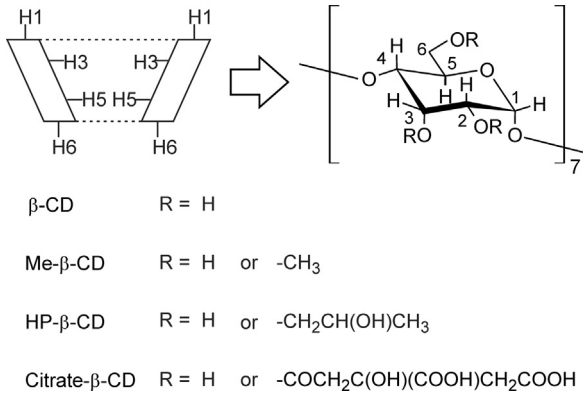

Scheme 2. Chemical structures of the β-cyclodextrins used in this study.

Vasconi, Hinrichsen & Lamas, 2014): ABZ (0.56 mmol) and the cyclodextrin (0.56 mmol) were dissolved in 30 mL of acetic acid (30% v/v). Each resulting solution was spray-dried using a Mini Spray Dryer Buchi B-290 (Flawil, Switzerland) under the following conditions: inlet temperature: 130 °C, outlet temperature: 70 °C, air flow: 38 m^3/h, feed: 5 mL/min and aspirator set: 100%.

2.2.2. ^{13}C and ^{15}N solid-state NMR studies

Powdered samples of ABZ and ABZ:CDs (~200 mg) were packed into 7 mm o.d. cylindrical zirconia rotors. ^{13}C cross polarization/magic angle spinning (CP/MAS) and ^{15}N CP/MAS spectra were obtained at 75.49 MHz and 30.42 MHz, respectively, on a Tecmag Redstone/Bruker 300 WB spectrometer, at a MAS rate of 3.5 kHz, with 90° RF pulses of about 4 μs and 6 μs, contact time of 100 μs or 3 ms, and relaxation delay of 5 s and 15 s, respectively. The significant contributions of the ^{13}C spinning side bands, particularly in the aromatic and carbonyl regions, were suppressed by running the spectra with the SELTICS sequence (Sideband Elimination by Temporary Interruption of Chemical Shift (Hong & Harbison, 1993). CP/MAS spectra with removal of ^{13}C non-quaternary signals was achieved by interrupting proton decoupling during 40 μs before the acquisition period. ^{13}C and ^{15}N chemical shifts were referenced with respect to external glycine (^{13}CO observed at 176.03 ppm and $^{15}NH_2$ observed at 32.4 ppm in the liquid NH_3 scale).

3. Results and discussion

The chemical structures of the β-CDs evaluated in this study aiming to improve ABZ solubility are depicted in Scheme 2. The ^{13}C CP/MAS spectra obtained from β-CD, Me-β-CD, HP-β-CD and citrate-β-CD (Fig. 1) show that narrower lines are obtained for β-CD

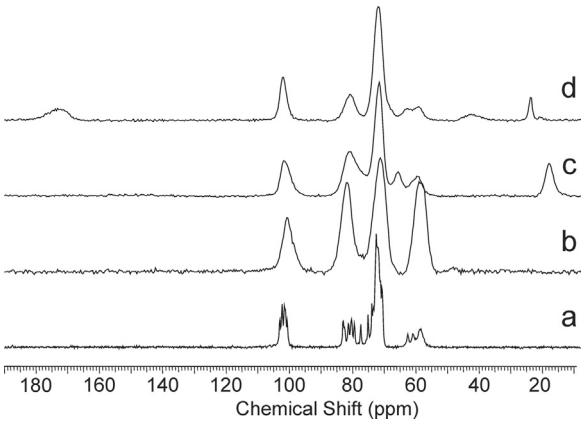

Fig. 1. ^{13}C CP/MAS spectra obtained from β-CD, Me-β-CD, HP-β-CD and citrate-β-CD (from a to d, respectively).

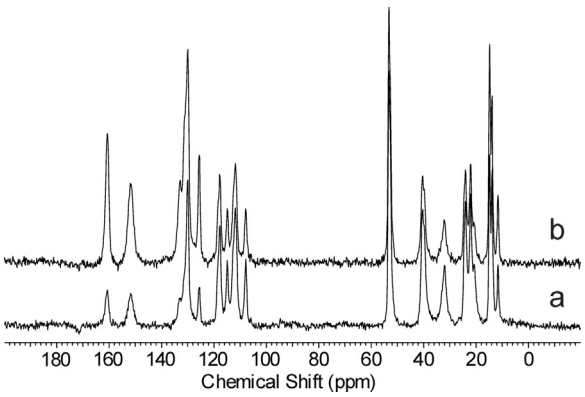

Fig. 2. ^{13}C CP/MAS spectra obtained from ABZ under 100 μs (a) and 3 ms (b) contact times, respectively.

resonances in comparison with the others CDs which is consistent with higher order at short distance in β-CD.

The β-CD spectrum is comparable to those earlier reported (e.g. Wulff, Aldén & Tegenfeldt, 2002). More than one signal was recorded from each β-CD carbon due to torsion angles relating to diverse orientations of hydroxyl groups and to the variety of torsion angles about the (1 > 4) linkages for C1 and C4 (Sfihi, Legrand, Doussot, & Guy, 1996). Broad lines recorded from Me-β-CD, HP-β-CD and citrate-β-CD reflect the presence of a distribution of local electronic shielding. ^{13}C chemical shifts of the CDs in pure states are shown in Table 1.

Fig. 2 shows typical ^{13}C CP/MAS spectra recorded from ABZ under different contact times: 100 μs and 3 ms. Table 2 presents the ^{13}C ABZ chemicals shifts. At a first observation, it is noticed that the ABZ spectrum is from a crystalline compound with more than one molecule in the asymmetric unit because more than one resonance is assigned to each carbon species. For example, three distinct C12 resonances are identified. The influence of duration of the ^{1}H to ^{13}C magnetization transfer (or cross polarization) on carbon signal intensities was evaluated to assist performing a full spectrum assignment. The comparison of spectral intensities displayed in Fig. 2a and b enables noticing that the most affected signals by shortening CP from 3 ms to 100 μs are from C1, C2, C3, C4, C5 and C6. This is expected for quaternary carbons but not for C6 because directly bonded hydrogen strongly favors ^{1}H-^{13}C CP. X-ray crystallography data on ABZ help explaining such result (Pranzo et al., 2010). As mentioned before, Form I is the commercialized ABZ, and therefore was the form used in the present study, but the only crystal structure reported on ABZ is from Form II. The latter is best described by the tautomer ae (Scheme 1) assuming 50% occupancy of positions C5 and C6 for the propylthioside chain. Spectral ss-NMR data now suggest that the propylthioside chain can indeed be found at two different positions in Form I. NMR data also indicate order at short distance (not determined by X-ray crystallography, which depends on long distance order). It is not clear however if Form I is better described by tautomer ae as in Form II or if it is a mixture of all three tautomers (a, e and ae in Scheme 1). The ^{15}N broad resonance from the benzimidazole ring (Fig. 4) is consistent with disorder in protonated nitrogen atoms, but at present, it is not possible to conclude unequivocally either about the protonation degree (one or two protonated nitrogen atoms) or on the protonated nitrogen (as shown in Scheme 1).

Unlike pure ABZ, samples containing mixtures of ABZ and cyclodextrins are amorphous, as evidenced by broad ABZ and all cyclodextrin signals in the ^{13}C CP/MAS spectra shown in Fig. 3, which also display the pure ABZ spectrum for comparison (chemical shifts are presented in Table 2). This is consistent with previous results that showed that the samples are amorphous by powder X-ray diffraction, and partially explains the success of the spray-drying technique in producing solids that have better dissolution rates then ABZ, since the technique provides a way of destroying the crystalline form interactions (García, Leonardi, Salazar et al., 2014a).

The ABZ signals from C3, C4, C5 and C6 collapse into two broad signals (with different intensities) in all ABZ:CD spectra except for ABZ:citrate-β-CD, in which case just one very broad peak is displayed; a similar remark applies to resonances in the range

Table 1
^{13}C CP/MAS chemicals shifts (δ/ppm) obtained from β-CD, Me-β-CD, HP-β-CD and citrate-β-CD.

Cyclodextrin	Carbon number				Group substituent
	1	2,3,5	4	6	
β-CD	103.7 to 101.5 (102.64)[a]	76.1–71.7 (72.17)[a]	82.3–78.3 (81.60)[a]	63.6–59.4 (60.77)[a]	–
Me-β-CD	101.8	71.9	83.0	59.4	**—CH_3** 59.4
HP-β-CD	102.9	72.9	81.8	63.9[b], 60.3[b]	**—$OCH_2C(OH)CH_3$** CH_2:~72 C:66.9, CH_3:19.3
Citrate-β-CD	102.9	72.9	81.9	62[c]	**—$CO_2C(CH_2)_2(CO_2H)_2OH$** CO: 168–183[c] C:64.1, CH_2:44.2[c] 25.0[d], 22[d]

[a] (Wulff et al., 2002).
[b] Superimposed.
[c] Broad.
[d] Not assigned

Table 2
^{13}C CP/MAS and ^{15}N CP/MAS chemical shifts (δ/ppm) obtained from ABZ, ABZ:β-CD, ABZ:Me-β-CD, ABZ:HP-β-CD and ABZ:citrate-β-CD.

Carbon number	^{13}C				
	ABZ	ABZ:β-CD	ABZ:Me-β-CD	ABZ:HP-β-CD	ABZ:citrate-β-CD
1	160.81	174.99[a]	173.4[a]	175.3[a]	162.19[b]
		162.54	162.0	162.5	
2	151.82[c]	156.14[d]	155.10	155.96	153.02
		153.02	149.05	149.05	150.8[d]
3	132.96	131.75	140.22	140.22	131.4[e]
			132.44	132.09	
4	131.23				
5	130.02	128.81[d]	127.94	128.29	128.5[e]
6	125.69				
7	117.74	117.2–107.8	116.87[e]	117.9[e]	117–111[e]
	111.86[c]				
8	114.97		111.85[e]	–	
	107.88[c]				
9	53.21, 52.87[d]	52.18	52.87, 49.06[d]	52.70	52.52
10	40.59, 39.90	38.51	39.03	38.68	38.51[d]
11	32.11[c], 24.50[d]	32.46[c]	22.25	33.32[c,d]	32.46[c,e]
	24.15, 22.08, 20.87	22.25	21.56	22.25[d]	21.04
		20.87	20.69		
12	14.81, 13.95, 11.70	13.95	12.91	13.95	13.26
Group	^{15}N				
imidazole	150[e]	–	–	–	–
carbamate	125.1	133.94	129.5	125.5	133.14
		124.71	125.1, 103.44		124.31

[a] Residual acetic acid.
[b] Other carbonyl signals overlap with citrate fragment resonances.
[c] Broad.
[d] Shoulder.
[e] Tentative assignment.

107–118 ppm, assigned to C7 and C8 to all samples but ABZ:β-CD (signals are partially resolved in this case). Based on the similarity of ^{13}C ABZ signals recorded in the 135–158 ppm range (Fig. 3), it is worth mentioning that ABZ:CDs may be divided into two groups: (1) ABZ:Me-β-CD and ABZ:HP-β-CD, (2) ABZ:β-CD and ABZ:citrate-β-CD. This association is more evident from ^{15}N data (Fig. 4, chemical shifts are summarized in Table 2) because both ABZ:β-CD and ABZ:citrate-β-CD spectra display a signal at about 133 ppm (more intense in the ABZ:citrate-β-CD spectrum). Such resonances that may be assigned to carbamate NH groups involved in hydrogen bonding were not recorded either from ABZ:Me-β-CD or from ABZ:HP-β-CD. This is consistent with the dissolution rate study previously reported (García, Leonardi, Salazar et al., 2014a).

ABZ:Me-β-CD and ABZ:HP-β-CD display similar ABZ signals (Fig. 3) with just slight relative intensity differences and a small high-field shift of C12 resonance for ABZ:Me-β-CD. Two signals assigned to C2 in ABZ:Me-β-CD and ABZ:HP-β-CD spectra (at about 155 and 149 ppm) are consistent with the presence of ABZ molecules with different C2 electronic environments. Such chemical shift differences cannot be explained by the presence of different conformers and are probably associated with different tautomers, since this carbon is directly bond to three nitrogens (Scheme 1). This is supported by the new signal appearing at 103.44 ppm in the ^{15}N ABZ:Me-β-CD spectrum (Fig. 4) that is tentatively assigned to N10 in tautomer ae shown in Scheme 1 (the signal to noise ratio in ABZ:HP-β-CD spectrum precludes any signal identification in the same frequency range). When compared to free ABZ these two mixtures show major ^{13}C spectral differences in the aromatic region and for C1 that appears here at about 162 ppm, that is 1 ppm shifted to lower magnetic field. There is therefore the possibility

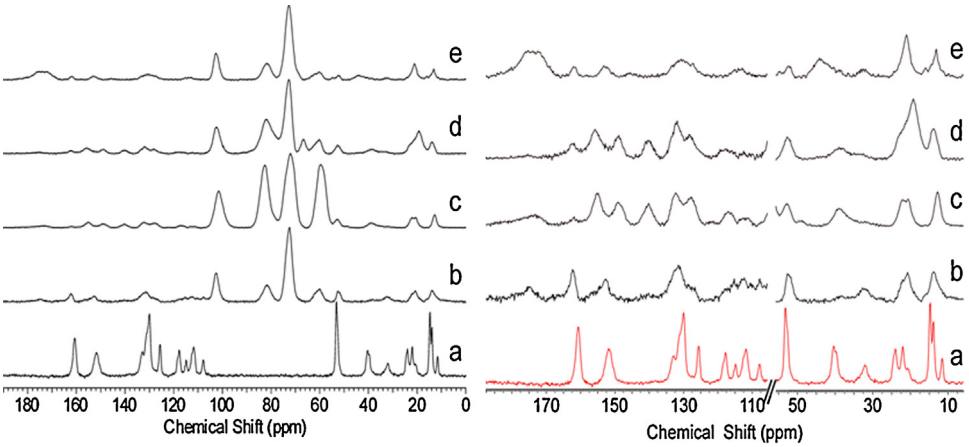

Fig. 3. Left side: full ^{13}C spectra obtained from ABZ, ABZ: β-CD, ABZ:Me-β-CD, ABZ:HP-β-CD and ABZ:citrate-β-CD (from a to e, respectively) under CP/MAS with 3 ms contact time. Right side: selected chemical shift ranges plotted here with expanded vertical scale; red lines display the free ABZ spectrum (For interpretation of the references to color in this figure legend, the reader is referred to the web version of this article.).

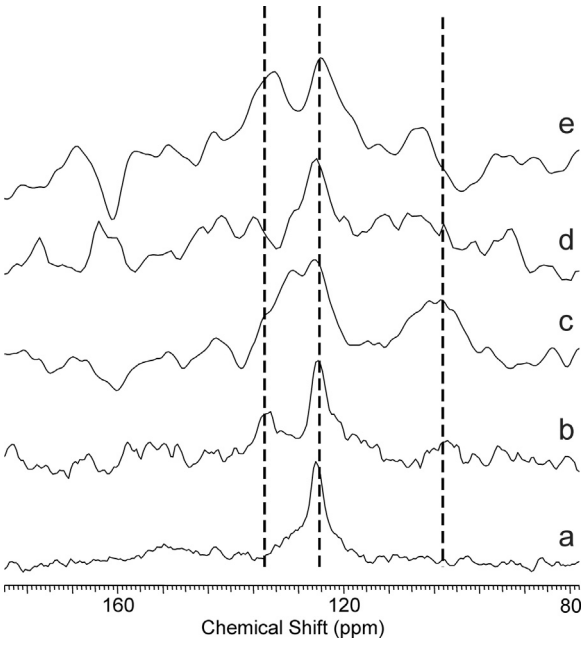

Fig. 4. ^{15}N CP/MAS spectra obtained from ABZ, ABZ: β-CD, ABZ:Me-β-CD, ABZ:HP-β-CD and ABZ:citrate-β-CD samples (from a to e, respectively). Dashed lines are just guides to the eyes.

that in these samples the carbamate has a hydrogen bridge to an OH, possibly to a CD-OH. Such result does not allow to unequivocally concluding about the presence of inclusion complexes because NMR data may be assigned to ABZ:CD complexes with different rearrangements: (a) ABZ inside the CD cavity, taking into consideration the diversity of probable conformations (some are shown in Scheme 1), (b) ABZ outside the CD cavity, with various probable orientations towards the toroid structure, for example with carbonyl groups linked by hydrogen bonds to CD hydroxyls.

^{13}C CP/MAS spectrum of β-CD display well resolved signals as expected from a crystalline compound (Fig. 1). The resonances arising from the ABZ:β-CD spray-dried sample are broad, featureless, which implies that the crystalline nature of β-CD has been lost. There are also significant changes in the β-CD signals: peaks at 78.30 ppm and 76.05 ppm are absent, and resonances at 83.8 ppm at 63.6 ppm show an intensity decrease. However, the resonance envelopes remain at about 81.8 ppm (C1) and about 61 ppm (C6). The signals assigned to ABZ in ABZ:β-CD are also broad. The following major differences are noticed when compared to the ABZ spectrum: (a) signals at 125.69 ppm, 53.21 ppm and 25.15 ppm are missing, (b) resonances at 52.18 ppm, 38.51 ppm, 13.95 ppm became broad, (c) C1 resonance (from ABZ) shifts to lower magnetic field (from 160.81 to 162.54 ppm).

The spectrum appears to have contributions from two different types of ABZ. The major species has some similarities to the species found in ABZ:Me-β-CD and ABZ:HP-β-CD, the major differences being the inversion of intensities in the signals at around 30 and 40 ppm, as well as the chemical shifts of the signals attributed to C2 and C3. The signal observed at about 175 ppm was assigned to residual acetic acid (see the Materials and methods section for details).

ABZ:β-CD and ABZ:citrate-β-CD spectra do show similar features, like chemical shifts assigned to C1 and C2. There are also some differences between these two spectra: two asymmetric broad (overlapping) ABZ:β-CD signals are observed in the region 120–130 ppm and one ABZ:citrate-β-CD broad resonance, and the signals at 117.74, 114.97, 111.86 and 107.88 ppm in pure ABZ spectrum are collapsed into one ABZ:citrate-β-CD broad signal but remain partially resolved in ABZ:β-CD spectrum (as already pointed out). The latter observation is consistent with these systems undergoing motion in different mobility scales.

ABZ:citrate-β-CD is in solution a stable inclusion complex (García, Leonardi, Salazar et al., 2014a). By comparing the ABZ:citrate-β-CD and citrate-β-CD spectra, is noticed that the signal at 64.1 ppm is not observed in the presence of ABZ (citrate fragment quaternary carbon) which can point to a strong and stable interaction between citrate-β-CD and ABZ also in the solid state, most possibly in the form of an inclusion complex.

Overall, it may be concluded that the ABZ high solubility enhancement in the form of an ABZ:citrate-β-CD inclusion complex is explained by the presence of one single highly stable species, which although being identified in ABZ:β-CD samples is not the unique species present in this system. This is consistent with the previous finding that ABZ has 15.3 times more affinity to citrate-β-CD than to β-CD (García, Leonardi, Salazar et al., 2014a). As far as ABZ:Me-β-CD and ABZ:HP-β-CD are concerned, differences in chemical shifts found between the isolated compounds and the mixture suggest some interaction but weaker than in the ABZ sample prepared with citrate-β-CD. More than one species was identified, which may be assigned to complexes with ABZ distinct structures. It is worth mentioning that, when compared with a suspension dosage form in mice, a weak ABZ:HP-β-CD binary complex was found to increase the relative bioavailability by only 40% (Castillo et al., 1999).

Probing if the inclusion complex found for ABZ:citrate-β-CD in the solid state was the one previously identified in solution (García, Leonardi, Salazar et al., 2014a) will be difficult. As pointed out (Wenz, 1994) substrates complexed with CD are in a very heterogeneous environment and complexed and free molecules may undergo fast exchange processes. Future work includes the evaluation of the stability of the ABZ:citrate-β-CD inclusion complex as previously described for a cholesterol-lowering drug (Nunes et al., 2014). This study will be performed by probing mobility in the kHz frequency range through spin-lattice relaxation time in the rotating frame measurements as a function of temperature.

4. Conclusions

Solid-state ^{13}C and ^{15}N NMR studies on ABZ and β-CDs spray-dried samples presented evidence for chemical interaction between ABZ and β-CDs which depends clearly on the β-CD substituent. For CDs with higher hydrophobic cavity (Me-β-CD and HP-β-CD) different ABZ tautomers appear to be present. Samples of ABZ with β-CD and citrate-β-CD have spectral data suggesting the formation of inclusion complexes, which are the dominant species for ABZ:citrate-β-CD. Solid-state NMR data has contributed therefore to explain the differences in ABZ solubility enhancement found with the different CDs.

Acknowledgments

The authors express their gratitude to “Fundação para a Ciência e a Tecnologia—Portugal” (project RECI/QEQ-QIN/0189/2012) for the financial support. A.G. is grateful to CONICET (Consejo Nacional de Investigaciones Científicas y Técnicas) for a Doctoral Fellowship. The authors also gratefully acknowledge the Universidad Nacional de Rosario and CONICET (Project no. PIP 112-201001-00194) for the financial support.

References

Ahmadnia, S., Moazeni, M., Mohammadi-Samani, S., & Oryan, A. (2013). In vivo evaluation of the efficacy of albendazole sulfoxide and albendazole sulfoxide loaded solid lipid nanoparticles against hydatid cyst. *Experimental Parasitology*, *135*(2), 314–319.

Barrera, M. G., Leonardi, D., Bolmaro, R. E., Echenique, C. G., Olivieri, A. C., Salomon, C. J., & Lamas, M. C. (2010). In vivo evaluation of albendazole microspheres for the treatment of Toxocara canis larva migrans. *European Journal of Pharmaceutics and Biopharmaceutics*, *75*(3), 451–454.

Brewster, M. E., & Loftsson, T. (2007). Cyclodextrins as pharmaceutical solubilizers. *Advanced Drug Delivery Reviews*, *59*(7), 645–666.

Carrier, R. L., Miller, L. A., & Ahmed, I. (2007). The utility of cyclodextrins for enhancing oral bioavailability. *Journal of Controlled Release*, *123*(2), 78–99.

Castillo, J. A., Palomo-Canales, J., Garcia, J. J., Lastres, J. L., Bolas, F., & Torrado, J. J. (1999). Preparation and characterization of albendazole β-cyclodextrin complexes. *Drug Development and Industrial Pharmacy*, *25*, 1241–1248.

Cook, G. C. (1990). Use of benzimidazole chemotherapy in human helminthiases: Indications and efficacy. *Parasitology Today*, *6*(4), 133–136.

Fernández, L., Sigal, E., Otero, L., Silber, J. J., & Santo, M. (2011). Solubility improvement of an anthelmintic benzimidazole carbamate by association with dendrimers. *Brazilian Journal of Chemical Engineering*, *28*(4), 679–689.

García, A., Barrera, M. G., Piccirilli, G., Vasconi, M. D., Di Masso, R. J., Leonardi, D., et al. (2013). Novel albendazole formulations given during the intestinal phase of *Trichinella spiralis* infection reduce effectively parasitic muscle burden in mice. *Parasitology International*, *62*(6), 568–570.

García, A., Leonardi, D., Salazar, M. O., & Lamas, M. C. (2014). Modified β-Cyclodextrin inclusion complex to improve the physicochemical properties of albendazole. Complete in vitro evaluation and characterization. *PLoS One*, *9*(2), e88234.

García, A., Leonardi, D., Vasconi, M. D., Hinrichsen, L. I., & Lamas, M. C. (2014). Characterization of albendazole-randomly methylated β-cyclodextrin inclusion complex and in vivo evaluation of its antihelmitic activity in a murine model of trichinellosis. *PLoS One*, *9*(11), e113296.

García, J. J., Bolás, F., & Torrado, J. J. (2003). Bioavailability and efficacy characteristics of two different oral liquid formulations of albendazole. *International Journal of Pharmaceutics*, *250*(2), 351–358.

Hong, J., & Harbison, G. S. (1993). Magic-angle spinning sideband elimination by temporary interruption of the chemical shift. *Journal of Magnetic Resonance, Series A*, *105*(2), 128–136.

Kohri, N., Yamayoshi, Y., Iseki, K., Sato, N., Todo, S., & Miyazaki, K. (1998). Effect of gastric pH on the bioavailability of albendazole. *Pharmacy and Pharmacology Communications*, *4*, 267–270.

Lopez-Garcia, M. L., Torrado-Duran, S., Torrado-Duran, J., Martínez-Fernández, A. R., & Bolás-Fernández, F. (1997). Albendazole versus ricobendazole (albendazole-sulphoxide) against enteral and parenteral stages of *Trichinella spiralis* in mice. *International Journal for Parasitology*, *27*(7), 781–785.

Nunes, T. G., Viciosa, M. T., Correia, N. T., Danède, F., Nunes, R. G., & Diogo, H. P. (2014). A stable amorphous statin: Solid-state NMR and dielectric studies on dynamic heterogeneity of simvastatin. *Molecular Pharmaceutics*, *11*, 727–737.

Paradowska, K., & Wawer, I. (2014). Solid-state NMR in the analysis of drugs and naturally occurring materials. *Journal of Pharmaceutical and Biomedical Analysis*, *93*, 27–42.

Pranzo, M. B., Cruickshank, D., Coruzzi, M., Caira, M. R., & Bettini, R. (2010). Enantiotropically related albendazole polymorphs. *Journal of Pharmaceutical Sciences*, *99*(9), 3731–3742.

Sfihi, H., Legrand, A. P., Doussot, J., & Guy, A. (1996). Solid-state 13C NMR study of β-cyclodextrin/substituted aromatic ketone complexes: Evidence for two kinds of complexation of the guest molecules. *Colloids and Surfaces A: Physicochemical and Engineering Aspects*, *115*(0), 115–126.

Vogt, F. G., & Strohmeier, M. (2012). 2D solid-state NMR analysis of inclusion in drug–cyclodextrin complexes. *Molecular Pharmaceutics*, *9*(11), 3357–3374.

Wenz, G. (1994). Cyclodextrins as building blocks for supramolecular structures and functional units. *Angewandte Chemie International Edition in English*, *33*, 803–822.

Wulff, M., Aldén, M., & Tegenfeldt, J. (2002). Solid-state NMR investigation of indomethacin cyclodextrin complexes in PEG6000 carrier. *Bioconjugate Chemistry*, *13*, 240–248.